A Letters Journal Exploring the Frontiers of Physics

January 2012

EPL, **97** (2012) 26002
doi: 10.1209/0295-5075/97/26002

www.epljournal.org

Mechanics of hierarchical 3-D nanofoams

Q. Chen[1,2] and N. M. Pugno[1,2,3,4(a)]

[1] *Department of Structural Engineering and Geotechnics, Politecnico di Torino - I-10129, Torino, Italy, EU*
[2] *Laboratory of Bio-Inspired Nanomechanics "Giuseppe Maria Pugno", Department of Structural Engineering and Geotechnics, Politecnico di Torino - I-10129, Torino, Italy, EU*
[3] *National Institute of Nuclear Physics, National Laboratories of Frascati - Via E. Fermi 40, I-00044, Frascati, Italy, EU*
[4] *National Institute of Metrological Research - Strada delle Cacce 91, I-10135, Torino, Italy, EU*

received 29 July 2011; accepted in final form 28 November 2011
published online 5 January 2012

PACS 61.46.-w – Structure of nanoscale materials
PACS 62.20.de – Elastic moduli
PACS 62.20.M- – Structural failure of materials

Abstract – In this paper, we study the mechanics of new three-dimensional hierarchical open-cell foams, and, in particular, its Young's modulus and plastic strength. We incorporate the effects of the surface elasticity and surface residual stress in the linear elastic and plastic analyses. The results show that, as the cross-sectional dimension decreases, the influences of the surface effect on Young's modulus and plastic strength increase, and the surface effect makes the solid stiffer and stronger; similarly, as level n increases, these quantities approach to those of the classical theory as lower bounds.

Introduction. – The microstructure of materials plays an important role in determining their mechanical properties. In particular biological materials, *e.g.* bone and wood [1], display sophisticated hierarchical structures with different length scales and they have attractive mechanical performances, *e.g.* their toughness [2,3]. These outstanding properties of all hierarchical structures at different length scales are generating enormous interest. In this regard, the toughening mechanisms in nacre have been extensively studied [3,4] and recently, two theoretical models [5–7] were brought forward to investigate the mechanical properties of bone-like materials and spider silk. Up to now, engineers and scientists created only a few hierarchical structures. For example, the Eiffel Tower is considered as a three levels structure [8]; Geim *et al.* [9] developed arrays of microfabricated polyimide hairs to mimic the adhesive and self-cleaning properties of gecko's feet; Munch *et al.* [10] synthesized a bio-inspired hybrid material, and its toughness is more than 300 higher than that of constituent materials.

Foam structures (*e.g.* animal quill and plant stems), on the one hand, are often found in Nature, and they provide animals and plants with low weight, high strength etc.; biomimicking of the foam structures may offer the potential to increase the mechanical efficiency of engineering materials [11]. On the other hand, varieties of artificial open-cell foams are studied widely, and Biener *et al.* [12] combined nanoindentation, column microcompression and molecular dynamics simulations to study the mechanical behavior of nanoporous Au; they found nanoporous Au can be as strong as bulk Au, despite possessing high porosity; Wang and Xia [13] investigated the mechanical properties of hierarchical nanoporous solids, and found that the Young's modulus of the nanostructure is intrinsically size-dependent when considering the surface effect. The surface effect, due to the high surface-to-volume ratio [14], plays an important role in determining the mechanical properties of nanosystems. Extensive works [15–18] studied its influence on linear elastic and plastic properties; in some cases, the surface effect stiffens materials; while in others softens [19]. In particular, considering the surface energy of nanostructured materials with negative radius of curvature, including nanocavities, nanotubes and shell-core nanostructures, Ouyang *et al.* [20] reviewed the status and recent progress on their thermodynamic behavior (e.g. nonlinear shrinkage).

In this paper, inspired by biological materials, we build three-dimensional hierarchical foam (fig. 1) [13,21–26], and incorporating surface effect at each hierarchical level, we study its linear-elastic and plastic behaviors. Here, we

(a) E-mail: nicola.pugno@polito.it

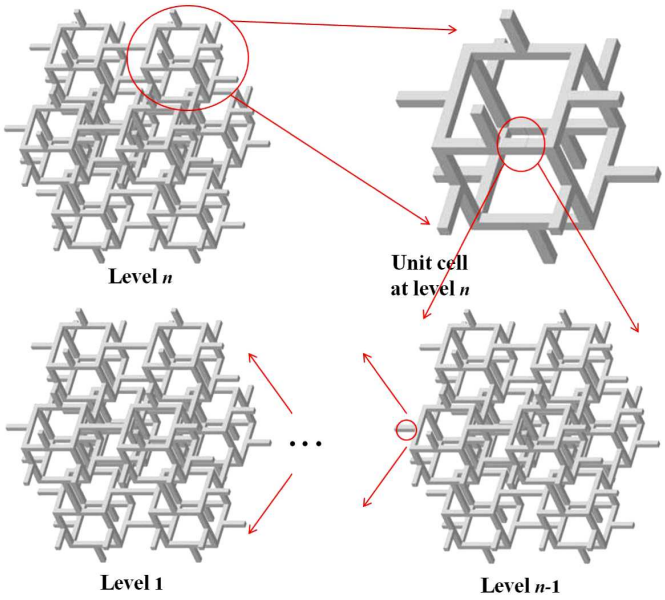

Fig. 1: (Colour on-line) Schematic of hierarchical foam.

include the effect of surface elasticity in the linear elastic analysis and the effect of the surface residual stress in the plastic analysis, respectively. Finally, considering a three-level hierarchy as an example, we analyze the mechanical properties at each hierarchical level.

Surface effect. – Surfaces of solids, possessing atoms with fewer neighbor atoms, display an excess energy with respect to the bulk; especially in nanostructures, the surface effect, including surface residual stress and surface elasticity, is an important property of solid surfaces [27]. The surface effect was first defined by Gibbs [28], and later, Cammarata [14] expressed the classical surface stress $\sigma^s_{\alpha\beta}$ as $\sigma^s_{\alpha\beta} = \gamma\delta_{\alpha\beta} + \partial\gamma/\partial\varepsilon^s_{\alpha\beta}$, where, γ is the surface energy, $\delta_{\alpha\beta}$ is the Kronecker delta, $\sigma^s_{\alpha\beta}$ and $\varepsilon^s_{\alpha\beta}$ are the surface stress and strain tensors, respectively. The expression suggests that the surface energy of nanostructures plays an important role in determining the surface stress. Regarding the relationship between Young's modulus and surface energy, Ouyang *et al.*, [29], basing on the thermodynamics and continuum medium mechanics, studied the correlation between Young's modulus and surface energy; they focused on carbon nanotubes, explaining the anomalous behavior of Young's modulus.

In particular, for the one-dimensional linear elastic case, $\sigma^s_{\alpha\beta}$ becomes [15]: $\sigma^s = \tau + E^s\varepsilon$ with $E^s = E^* t$, where, τ is the surface residual stress, E^s is the surface Young's modulus, E^* is Young's modulus of the surface layer and t is the thickness.

Young's modulus. –

First level. For the first level, the hierarchical foam (fig. 2) is conventional. Under the external stress σ (fig. 2(c)), the linear-elastic deformation includes the bending of beam 1, and the axial deformations of beams 2 and 3. On the one hand, assuming the clamped-clamped boundary condition of beam 1 and small deformations, the displacement due to the bending of beam 1 is

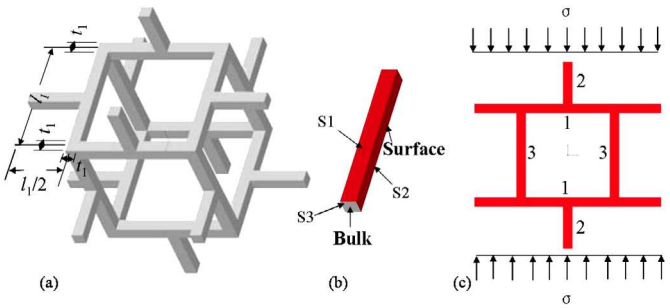

Fig. 2: (Colour on-line) (a) Unit cell at the first level. (b) Representative of ribs. (c) External stress acting on the unit cell.

$$\Delta' = 2 \times \frac{F/2 \cdot l_1^3}{192(EI)_1^e}, \tag{1}$$

where, $F = 4\sigma l_1^2$, Δ' is the mid-point displacement of the beam 1, F and σ are, respectively, the equivalent concentrated force and the external stress acting on the unit cell, l_1 is the rib length, $(EI)_1^e = E_0 t_1^4/12 + 2E_0^s t_1^3/3$ is the effective bending rigidity including the surface elasticity, where, E_0 and E_0^s are the bulk and surface Young's moduli, respectively, and t_1 is the side length of the square cross-section of the ribs at the first level.

Alternatively, from the expression of $(EI)_1^e$, the dimensionless Young's modulus E_0^e/E_0 can be derived as $E_0^e/E_0 = 1 + 8E_0^s/(\mathrm{E}_0 t_1)$. It coincides with the result by [30], and it obeys the scaling law $E_0^e/E_0 = 1 + \alpha l_{\mathrm{in}}/t_1$ [31] with $l_{\mathrm{in}} = E_0^s/E_0$ and $\alpha = 8.0$. Note that l_{in} is an intrinsic material length, reflecting a condition under which surface effect plays an important role compared to bulk; α is a dimensionless constant, which depends on the geometry of structural elements (*e.g.* bar, plate, etc.) and their deformations (*e.g.* bending, tension, etc.).

Note that, eq. (1) is based on the Euler beam theory, which neglects the shear effect; if t_1/l_1 is not small enough, then, the shear effect has to be considered, *i.e.*, the Timoshenko beam theory holds.

On the other hand, the axial displacements due to the axial deformation of beam 2 and beam 3 are easily derived:

$$\begin{aligned} \Delta'' &= 2 \times \frac{F/2 \cdot l_1/2}{(EA)_1^e}, \\ \Delta''' &= \frac{F/4 \cdot l_1}{(EA)_1^e}, \end{aligned} \tag{2}$$

where, Δ'' and Δ''' are the displacements of beam 2 and 3, respectively, $(EA)_1^e$ is the effective longitudinal stiffness considering the surface elasticity and it is expressed as $(EA)_1^e = E_0 t_1^2 + 4E_0^s t_1$. Thus, the expression of $(EA)_1^e$ is rearranged as a dimensionless quantity: $E_0^e/E_0 = 1 + 4E_0^s/(\mathrm{E}_0 t_1)$.

Therefore, the total displacement is obtained by summing eqs. (1) and (2), *i.e.*, $\Delta_1 = \Delta' + \Delta'' + \Delta'''$. Meanwhile, considering $F = 4\sigma l_1^2$, we obtain

$$\Delta_1 = \frac{\sigma l_1^5}{48(EI)_1^e} + \frac{3\sigma l_1^3}{(EA)_1^e}, \tag{3}$$

thus, the strain ε_1 of the unit cell at the first level can be found:

$$\varepsilon_1 = \frac{\Delta_1}{2l_1} = \frac{\sigma l_1^4}{8(E_0 t_1^4 + 8E_0^s t_1^3)} + \frac{3\sigma l_1^2}{2(E_0 t_1^2 + 4E_0^s t_1)}. \tag{4}$$

Furthermore, Young's modulus of the first level is calculated by $E_1 = \sigma/\varepsilon_1$ and normalized by Young's modulus (E_0) of the solid; we have

$$\frac{E_1}{E_0} = \frac{8(t_1/l_1)^4(t_1 + 4\frac{E_0^s}{E_0})(t_1 + 8\frac{E_0^s}{E_0})}{t_1(t_1 + 4\frac{E_0^s}{E_0}) + 12(t_1/l_1)^2 t_1(t_1 + 8\frac{E_0^s}{E_0})}. \tag{5}$$

The geometry in fig. 2 gives a relative density: $\rho_1/\rho_0 = \frac{9}{4}(t_1/l_1)^2$. Accordingly, normalized Young's modulus E_1/E_0 is expressed through the relative density as

$$\frac{E_1}{E_0} = \frac{128(\rho_1/\rho_0)^2(t_1 + 4\frac{E_0^s}{E_0})(t_1 + 8\frac{E_0^s}{E_0})}{81t_1(t_1 + 4\frac{E_0^s}{E_0}) + 432(\rho_1/\rho_0)t_1(t_1 + 8\frac{E_0^s}{E_0})}. \tag{6}$$

If the rib size t_1 is large enough, then, the surface effect could be neglected ($E_0^s = 0$), and

$$\frac{E_1}{E_0} = \frac{128(\rho_1/\rho_0)^2}{81 + 432(\rho_1/\rho_0)}. \tag{7}$$

The expression (7) obeys $E_1/E_0 = (\rho_1/\rho_0)^2/[1 + \alpha(\rho_1/\rho_0)]$, which is a numerical result by curve fitting for three-dimensional open-cell foams basing on Voronoi models [32]. Therefore, with the effect of the surface elasticity, the normalized Young's modulus is expressed as the classical power law with respect to the relative density:

$$\frac{E_1}{E_0} = C_1 \left(\frac{\rho_1}{\rho_0}\right)^2 \quad \text{with}$$

$$C_1 = \frac{128(t_1 + 4\frac{E_0^s}{E_0})(t_1 + 8\frac{E_0^s}{E_0})}{\left[81t_1(t_1 + 4\frac{E_0^s}{E_0}) + 432(\rho_1/\rho_0)t_1(t_1 + 8\frac{E_0^s}{E_0})\right]}. \tag{8}$$

In addition to the above structural analysis, Ouyang *et al.* [33] predicted Young's modulus of nanoporous materials by employing the relationship between surface energy and Young's modulus, and finally investigated the influences of the porosity on the material Young's modulus.

Second level. For the second level, if the structure has a considerable large size compared with that of the first level, we could neglect the effect of the surface elasticity. However, in general, eq. (8) is employed as an iterative procedure and the normalized Young's modulus of the second level is calculated:

$$\frac{E_2}{E_0} = C_1 C_2 \cdot \left(\frac{\rho_2}{\rho_0}\right)^2, \tag{9}$$

where C_2 is calculated by replacements of the corresponding parameters of the second hierarchical level in the expression of C_1.

n-th level. Likewise, the normalized Young's modulus of the n-th level can be obtained:

$$\frac{E_n}{E_0} = \prod_{i=1}^{n} C_i \cdot \left(\frac{\rho_n}{\rho_0}\right)^2, \tag{10}$$

where, C_i are obtained through replacements of the corresponding parameters of level i in the expression of C_1.

Plastic strength. – As discussed in the introduction, hierarchical natural materials or structures exhibit high toughness, and this is because the crack path becomes longer along the different hierarchical levels; meanwhile, the hierarchical structures can inhibit the crack propagation at each level. In our case, we are not considering the presence of a matrix, thus we investigate the plastic strength of the hierarchical foam as main mechanism for energy dissipation. Here, we assume that ribs collapse in a fully plastic way, and the portion below the neutral axis is totally tensile yielded whereas that above the neutral axis is totally compressive yielded.

Effective yield strength. Like the elastic analysis, we only consider the influence of the surface residual stress on the plastic strength of the first level. Based on the von Mises yield condition, the effective initial yield strength in axial tension or on compression is expressed as [34,35]: $\sigma_e = \frac{\tau' + \tau''}{t_1} \pm \sqrt{\sigma_0^2 - \frac{3}{t_1^2}(\tau' - \tau'')^2}$, where, τ' and τ'' are surface residual stresses acting on surfaces 1 and 2 (fig. 2(b)), σ_0 is the yield strength of bulk materials and $\pm$ stands for tension (+) or compression (−) of the ribs, respectively.

First level. For the external stress, an upper bound on the plastic collapse stress could be calculated equating the work of the external force F to the plastic work of 12 plastic hinges (fig. 3(a), (b)), *i.e.*:

$$Fl_1\phi = 16M_p\phi \tag{11}$$

where, M_p is the plastic moment due to the yield (compression and tension) of all the cross-sectional area, ϕ is the rotating angle of the rib after that plastic hinges emerge.

Considering the surface residual stress, the cross-sectional stress distribution is shown in fig. 3(c)–(e). Besides, we define the surface thickness [36]: $h = nd$, where n is the number of atomic layers which displace a significant surface residual stress and can be determined by experiments or numerical analysis, and d is the characteristic size of atoms. Here the thickness is considered the same in all hierarchical levels. If h is much smaller than t_1, the neutral axis could still be considered in the

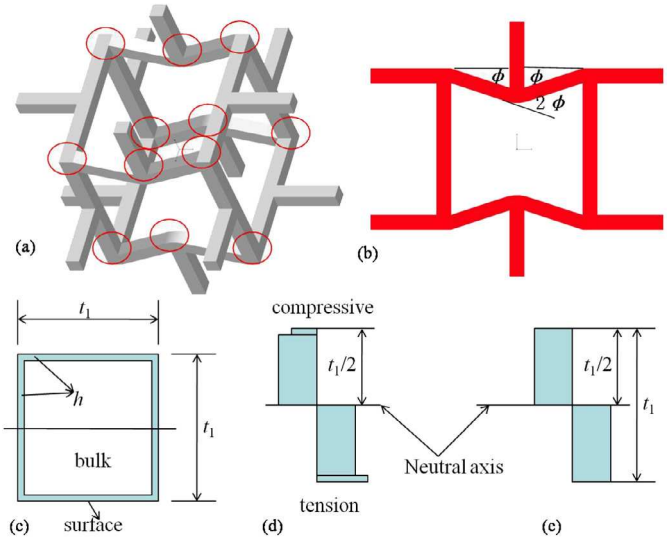

Fig. 3: (Colour on-line) (a) Twelve plastic hinges. (b) Rotation angles of the plastic hinges. (c) Core-shell model of surface effect. (d) Stress distribution with surface effect. (e) Stress distribution without surface effect.

middle of the cross-section (fig. 3(d), (e)). Then, M_p is calculated as:

$$M_p = \left(\frac{1}{4}\left(1-2\frac{h}{t_1}\right)^3+\sqrt{1-3\left(\frac{\tau'-\tau''}{\sigma_0 t_1}\right)} \cdot\frac{h}{t_1}\left(1+\frac{1}{2}\left(1-2\frac{h}{t_1}\right)^2\right)\right)\sigma_0 t_1^3, \tag{12}$$

substituting M_p and F into eq. (11), we have

$$\frac{\sigma_1}{\sigma_0} = \left(\left(1-2\frac{h}{t_1}\right)^3+2\sqrt{1-3\left(\frac{\tau'-\tau''}{\sigma_0 t_1}\right)} \cdot\frac{h}{t_1}\left(2+\left(1-2\frac{h}{t_1}\right)^2\right)\right)\cdot\left(\frac{t_1}{l_1}\right)^3. \tag{13}$$

Equation (13) is different from the Hall-Petch relationship, which is used to calculate the ligament yield strength of nanoporous Au foams influenced by the size effect [37]. On the other hand, a lower bound is obtained by equating the plastic moment M_p to the maximum bending moment $M_{\max}$ along the beam, *i.e.*:

$$M_p = M_{\max}, \tag{14}$$

where, $M_{\max} = \frac{1}{16}Fl_1$ is the maximum moment along the beam. Employing M_p (eq. (12)), we find

$$\frac{\sigma_1}{\sigma_0} = \left(\left(1-2\frac{h}{t_1}\right)^3+2\sqrt{1-3\left(\frac{\tau'-\tau''}{\sigma_0 t_1}\right)} \cdot\frac{h}{t_1}\left(2+\left(1-2\frac{h}{t_1}\right)^2\right)\right)\cdot\left(\frac{t_1}{l_1}\right)^3. \tag{15}$$

Equations (13) and (15) are the same, showing that the result represents the real value. The normalized strength of the first level is expressed by the relative density as

$$\frac{\sigma_1}{\sigma_0} = C_1'\left(\frac{\rho_1}{\rho_0}\right)^{3/2} \text{ with}$$
$$C_1' = 0.3\left(\left(1-2\frac{h}{t_1}\right)^3 +2\sqrt{1-3\left(\frac{\tau'-\tau''}{\sigma_0 t_1}\right)}\cdot\frac{h}{t_1}\left(2+\left(1-2\frac{h}{t_1}\right)^2\right)\right). \tag{16}$$

If the influence of the surface residual stress is negligible, the stress distribution will be like that reported in fig. 3(e) and the yield stress will be σ_0. Repeating the procedure or letting $\tau' = \tau'' = 0$ and $h = 0$, we have: $\sigma_1/\sigma_0 = 0.3(\rho_1/\rho_0)^{3/2}$, and this is a power law. Note that, the coefficient 0.3 was obtained by experimental fitting [21]; here, our derivation provides a theoretical proof.

n-th level. Like in the linear elastic analysis, the plastic strength of the n-th level can be derived as

$$\frac{\sigma_n}{\sigma_0} = \prod_{i=1}^{n} C_i' \cdot \left(\frac{\rho_n}{\rho_0}\right)^{3/2}, \tag{17}$$

where, C_i' are obtained through replacements of the corresponding parameters of level i in the expression of C_1'.

Analytic results. – In this section, since for higher levels the sizes of their structures are much larger than that of the first level, the surface effect can be neglected and we only consider the influence of the surface effect on the first level.

Firstly, for Young's modulus, we compare our predictions with the result by Wang and Xia [13] considering the first level of a conventional foam composed by the same material Au having $E_0 = 78\,\text{GPa}$, $E_s = 6.6\,\text{N/m}$ and $\rho_1/\rho_0 = 0.2$ [13,38]. The comparison is depicted in fig. 4(a). It shows that Young's modulus of our structure is 20% higher than calculated by Wang and Xia [13] because of the different nanostructure (the macro-mechanical properties of materials depend on their micro-structures). However, the influence of the surface effect is comparable.

Also, we investigate a three-level hierarchical structure with the same Au elastic constants stated above, while surface residual stresses $\tau' = \tau'' = 1.4\,\text{N/m}$ [27] on the (001) surface and yield strength $\sigma_0 = 1450\,\text{MPa}$ [39] are adopted. Also, for the plastic strength, we use $n = 3$, and $d_{\text{Au}} = 0.288\,\text{nm}$ and a ratio $t_i/l_i = 1/5$; the hierarchical structure is self-similar. Accordingly, the relative density is $\rho_{i+}1/\rho_i = 0.09$.

The analytic calculations of Young's modulus and plastic strength are reported in fig. 4(b), (c). They show that

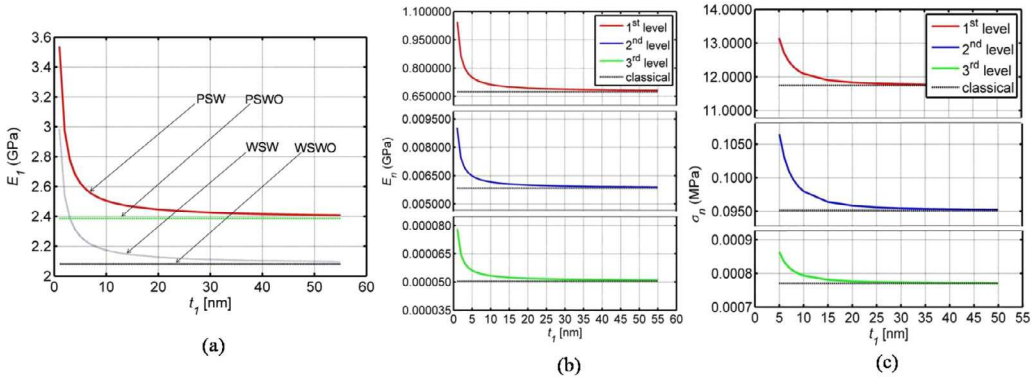

Fig. 4: (Colour on-line) (a) Comparison of Young's moduli between different nanostructures. (b) Young's modulus *vs.* t_1. (c) Plastic strength *vs.* t_1. Note: in (a), "PSW" or "PSWO" denote present structure with or without surface effect; "WSW" or "WSWO" denote Wang's structure with or without surface effect. In (b), (c), 1st (or 2nd, 3rd) level denote the results of the three-level hierarchical structure considering the surface effect; "classical" denotes the result calculated from classical theory without consideration of the surface effect.

the smaller t_1, the greater the influence on Young's modulus and strength and that, as t_1 increases, the predictions considering the surface effect approach those of the classical theory. Besides, our predictions including the surface effect are always higher than the classical ones; namely, the material becomes stiffer in the presence of the surface effect.

Conclusions. – This paper analytically derives Young's modulus and plastic strength for a three-dimensional hierarchical foam, considering the surface effect. Based on structural analysis, Young's modulus is derived with the effect of surface elasticity and the plastic strength with the effect of surface residual stress. We find that both Young's modulus and the plastic strength increase as the cross-sectional size t_1 of ribs at the first level decreases. This explains the important role of the surface effect in nanostructures. Thus, the present theory could be used to design some cellular nanomaterials for different applications, in addition to the recently developed hierarchical fibre bundle model [24,26].

* * *

NMP is supported by Regione Piemonte, METREGEN (2009–2012) "Metrology on a cellular and macromolecular scale for regenerative medicine".

REFERENCES

[1] Fratzl P. and Weinkamer R., *Prog. Mater. Sci.*, **52** (2007) 1263.
[2] Launey M. E. and Ritchie R. O., *Adv. Mater.*, **21** (2009) 2103.
[3] Smith B. L., Schaffer T. E., Viani M., Thompson J. B., Frederick N. A., Kindt J., Belcher A., Stucky G. D., Morse D. E. and Hansma P. K., *Nature*, **399** (1999) 761.
[4] Evans A. G., Suo Z., Wang R. Z., Aksay I. A., He M. Y. and Hutchinson J. W., *J. Mater. Res.*, **16** (2001) 2475.
[5] Gao H., *Int. J. Fract.*, **138** (2006) 101.
[6] Zhang Z., Zhang Y. and Gao H., *Proc. R. Soc. London, Ser. B*, **278** (2011) 519.
[7] Keten S., Xu Z., Ihle B. and Buehler M. J., *Nat. Mater.*, **9** (2010) 359.
[8] Lakes R., *Nature*, **361** (1993) 511.
[9] Geim A. K., Dubonos S. V., Grigorieva I. V., Novoselov K. S., Zhukov A. A. and Shapoval S. Y., *Nat. Mater.*, **2** (2003) 461.
[10] Munch E., Launey M. E., Alsem D. H., Saiz E., Tomsia A. P. and Ritchie R. O., *Science*, **322** (2008) 1516.
[11] Karam G. N. and Gibson L. J., *Mater. Sci. Eng. C*, **2** (1994) 113.
[12] Biener J., Hdoge A. M., Hayes J. R., Volkert C. A., Zepeda-Ruiz L. A., Hamza A. V. and Abraham F. F., *Nano Lett.*, **6** (2006) 2379.
[13] Wang X. S. and Xia R., *EPL*, **92** (2010) 16004.
[14] Cammarata R. C., *Prog. Surf. Sci.*, **46** (1994) 1.
[15] Wang G. F. and Feng X. Q., *Appl. Phys. Lett.*, **94** (2009) 141913.
[16] Shankar M. R. and King A. H., *Appl. Phys. Lett.*, **90** (2007) 141907.
[17] Wong E. W., Sheehan P. E. and Lieber C. M., *Science*, **277** (1997) 1972.
[18] Zhang W. J., Wang T. J. and Chen X., *Int. J. Plast.*, **26** (2010) 957.
[19] Zhou L. G. and Huang H., *Appl. Phys. Lett.*, **84** (2004) 1940.
[20] Ouyang G., Wang C. X. and Yang G. W., *Chem. Rev.*, **109** (2009) 4221.
[21] Gibson L. J. and Ashby M. F., *Cellular solids: Structure and Properties*, second edition (Cambridge University Press, Cambridge) 1997.
[22] Pugno N. M., *Nanotechnology*, **17** (2006) 5480.

[23] Pugno N. and Carpinteri A., *Philos. Mag. Lett.*, **88** (2008) 397.
[24] Pugno N., Bosia F. and Carpinteri A., *Small*, **4** (2008) 1044.
[25] Chen Q. and Pugno N., *Compos.: Part B*, **42** (2011) 2030.
[26] Bosia F., Pugno N. and Buehler M., *Phys. Rev. E*, **82** (2010) 056103.
[27] Shenoy V. B., *Phys. Rev. B*, **71** (2005) 094104.
[28] Gibbs J. W., *The Scientific Papers of J. Willard Gibbs, Thermodynamics*, Vol. **1**: *Thermodynamics* (Dover, New York) 1961.
[29] Ouyang G., Li X. L., Tan X. and Yang G. W., *Phys. Rev. B*, **76** (2007) 193406.
[30] Miller R. E. and Shenoy V. B., *Nanotechnology*, **11** (2000) 139.
[31] Wang J., Duan H. L., Huang Z. P. and Karihaloo B. L., *Proc. R. Soc. London, Ser. A*, **462** (2006) 1355.
[32] Gan Y. X., Chen C. and Shen Y. P., *Int. J. Solids Struct.*, **42** (2005) 6628.
[33] Ouyang G., Yang G. W., Sun C. Q. and Zhu W. G., *Small*, **4** (2008) 1359.
[34] Yang Z., Lu Z. and Zhao Y. P., *Comput. Mater. Sci.*, **46** (2009) 142.
[35] Gioia G. and Dai X., *J. Appl. Mech.*, **73** (2006) 254.
[36] Zheng X. P., Cao Y. P., Li B., Feng X. Q. and Wang G. F., *Nanotechnology*, **21** (2010) 205702.
[37] Hodge A. M., Biener J., Hayes J. R., Bythrow P. M., Volkert C. and Hamza A. V., *Acta Mater.*, **55** (2007) 1343.
[38] Kiely J. D. and Houston J. E., *Phys. Rev. B*, **57** (1998) 12588.
[39] Lee D., Wei X., Chen X., Zhao M., Jun S. C., Hone J., Herbert E. G., Oliver W. C. and Kysarj W., *Scr. Mater.*, **56** (2007) 437.